SPIRE Science Verification Review 3

RAL

Instrument Throughput

Document Number: SPIRE-RAL-REP-002977

Author(s)
Bruce Swinyard
Locke Spencer

Date
19th October 2007

Contents

1. Reference Documents 2
2. Introduction and scope 2
3. List of requirements that the test programme was designed to evaluate 2
4. Test results and conclusions 2
   4.1 List of tests carried out 2
   4.2 Subsystem requirements tested at instrument level and their verification status 3
   4.3 Instrument-level requirements and their verification status. 6
5. Open Issues and Anomalies 13
6. Recommendations for further data analysis and test 13

1. Reference Documents

RD1 Proposed RSRF for SPIRE Photometer	SPIRE-RAL-NOT-002962 v2.1
RD2 BDA Specification Document	SPIRE-JPL-PRJ-000456
RD3 Marc's spreadsheets	
RD4 SMEC and Spectrometer Performance	*J-PB/Trevor and David's SVR Doc*
RD5 Optical Performance	*Marc's SVR Doc*
RD6 SPIRE PFM Filter Configuration	HSO-CDF-NOT-000117
RD7 Multi-mode Characterisation of the SPIRE Instrument	*Glenn Laurent's note*

2. Introduction and scope

This report details the results on the measurement of the SPIRE photometer and spectrometer passband measurements and the overall instrument transmission. These results are based on the analysis of data from the PFM4 test campaign.

3. List of requirements that the test programme was designed to evaluate

Requirement Name	Description	Requirement
IRD-OPTP-R05	Throughput	The throughput of the photometer mirrors, filters, dichroics and baffles shall be greater than 0.27 over the instrument waveband. This includes losses due to manufacturing defects; surface finish and alignment tolerances.
IRD-OPTP-R07	Out of band radiation	The end to end filtering of the photometer shall control the out of band radiation to be no more than 10^{-3} for 40 cm-1 to 200 cm-1 10^{-6} for 200 cm-1 to 1000 cm-1 10^{-9} for 1000 cm-1 to 100000 cm-1 of the in-band telescope background radiation.
IRD-OPTS-R05	Theoretical throughput	The theoretical throughput of the spectrometer mirrors; filters; beam splitters and baffles shall be greater than 0.2 over the total instrument waveband including all losses due to manufacturing defects; surface finish and alignment tolerances.
IRD-DETP-R08	Spectral response	≥ 90% at the nominal edge frequencies of the appropriate passband
IRD-OPTS-R08	Out of band radiation	The end-to-end filtering of the spectrometer shall control the out of band radiation to be no more than 10^{-3} for 40 cm-1 to 200 cm-1 10^{-6} for 200 cm-1 to 1000 cm-1 10^{-9} for 1000 cm-1 to 100000 cm-1 of the in band telescope background radiation.

4. Test results and conclusions

4.1 List of tests carried out

Two basic types of test were carried out separately on the photometer and spectrometer sides of the instruments these are described in outline here.

Spectral passband measurements:

These were taken using the internal cold black body for the spectrometer and consisted of taking FTS scans of the CBB at a series of different temperatures. We report here on the comparison between the expected and measured bandpass shapes once the throughput (AΩ) has been taken into account. The band edges are reported in RD4

For the photometer the spectral passband was measured using the external FTS and the hot black body source. We report on these measurements here – details of the analysis are given in RD1.

Transmission and throughput:

The total transmission of the instrument is measured using a cold black body (CBB) that fills the instrument field of view. This can be varied in temperature and has a surface made of a polymer/crystal matrix measured to be >0.98 absorbing. By taking V-I curves with the CBB set to a series of temperatures the absorbed power onto the bolometers can be measured and compared to the expected power using a set of model assumptions for the instrument. This is discussed in section 3.3

Tests that have not been fully carried out are those concerned with testing the out of band rejection of the instrument and therefore neither IRD-OPTP-R07 or IRD-OPTS-R08 on the out of band rejection are addressed in this note although there is good evidence from the individual component measurements that this should not be a significant problem.

4.2 Subsystem requirements tested at instrument level and their verification status

IRD-DETP-R08 Detector Bandpass: The photometer requirements as listed in the Detector Subsystem Specification Document (RD2) are:

λ_b	**μm**	250	363	517
Design $\lambda o/\Delta\lambda$		3.00	3.18	3.00
λ_L **(50% points)**	**μm**	208.3 +/- 2.1	306.0 +/- 3.1	430.8 +/- 4.3
λ_U	**μm**	291.7 +/- 8.5	420.0 +/- 12.3	603.2 +/- 17.6
$\lambda o/\Delta\lambda$		3.00 +/- 0.39	3.18 +/- 0.45	3.00 +/- 0.39

The pixels measured are described in RD1. The full analysis of the individual results for each pixel has not yet been carried out except to run an automatic procedure to find the band limits, band centre and resolution. Here we summarise the results for each band, compare the measured and expected bandpasses and describe steps taken to resolve the differences.

PLW:

The measured average bandpass is shown in figure 3.2-1 below. The short wavelength cutoff is controlled by PDIC-2 and, as discussed below, is not in the position expected from the individual measurements of the components. Taking the averages of the band centres, 50% edges and resolutions from all the pixels we achieve the following:

Band centre:	512.7 ± 4.7 μm
Upper 50% Edge	614.0 ± 8.6 μm
Lower 50% Edge	410.9 ± 6.6 μm
Resolving power (50% edges)	2.63 ± 0.07
Resolving power (band integrated)	2.54 ± 0.17

We can see that the PLW band is not compliant with the original specification.

PMW

The measured average bandpass is shown in figure 3.2-1 below. The long wavelength cutoff is expected to be controlled by the waveguide cut-off. However, as discussed below, the PDIC-2 cut-off is not in the

expected position and it is this that controls the long wavelength cut-off as measured. The short wavelength cut off is controlled by PDIC-1 and, again discussed below, this too is not in the position expected from the measurements of the individual components. Taking the averages of the band centres, 50% edges and resolutions from all the pixels we achieve the following:

Band centre:	352.9 ± 3.2 μm
Upper 50% Edge	405.9 ± 4.8 μm
Lower 50% Edge	299.9 ± 2.9 μm
Resolving power (50% edges)	3.37 ± 0.21
Resolving power (band integrated)	3.33 ± 0.15

The PMW band is compliant with the original specification for resolving power but the band-centre is not as specified.

PSW

It is important to note that there is significant atmospheric absorption saturation within this band and artifacts are expected in the atmospheric removal due to division by zero and imperfect fit. The data processing attempts to minimize these errors however does not completely eliminate them.

Band centre:	250.7 ± 1.7 μm
Upper 50% Edge	294.8 ± 6.2 μm
Lower 50% Edge	206.7 ± 5.5 μm
Resolving power (50% edges)	3.08 ± 0.10
Resolving power (band integrated)	2.89 ± 0.40*

*This value is highly dubious as there is a large variation in the band integrated width due to residuals from the atmospheric removal process.

PSW is fully compliant with the specification.

Spectral edges

Figure 3.2-1 shows the measured photometer bandpasses together with the bandpasses expected from individual measurements of the components. To construct the expected values we have altered the positions of the dichroic edges by shift the measured data with respect to the wavenumber grid. We have done this to make the expected fit the measured as it is clear that the measured positions of the high frequency edge of PLW; the low frequency edge of PM; the high frequency edge of PMW and the low frequency edge of PSW are significantly different from the expected values measured for the dichroics.

The original dichroic measured bandpasses (PDIC 1 and PDIC 2) have been shifted by approximately:

PDIC 2 transmission shifted ~0.76 cm-1
PDIC 2 reflection shifted ~1.01 cm-1
PDIC 1 transmission shifted ~0.71 cm-1
PDIC 1 reflection shifted ~1.01 cm-1

We propose from now on to us the stacked profiles with these shifts as the calibration data for the SPIRE photometer bandpasses (see RD1).

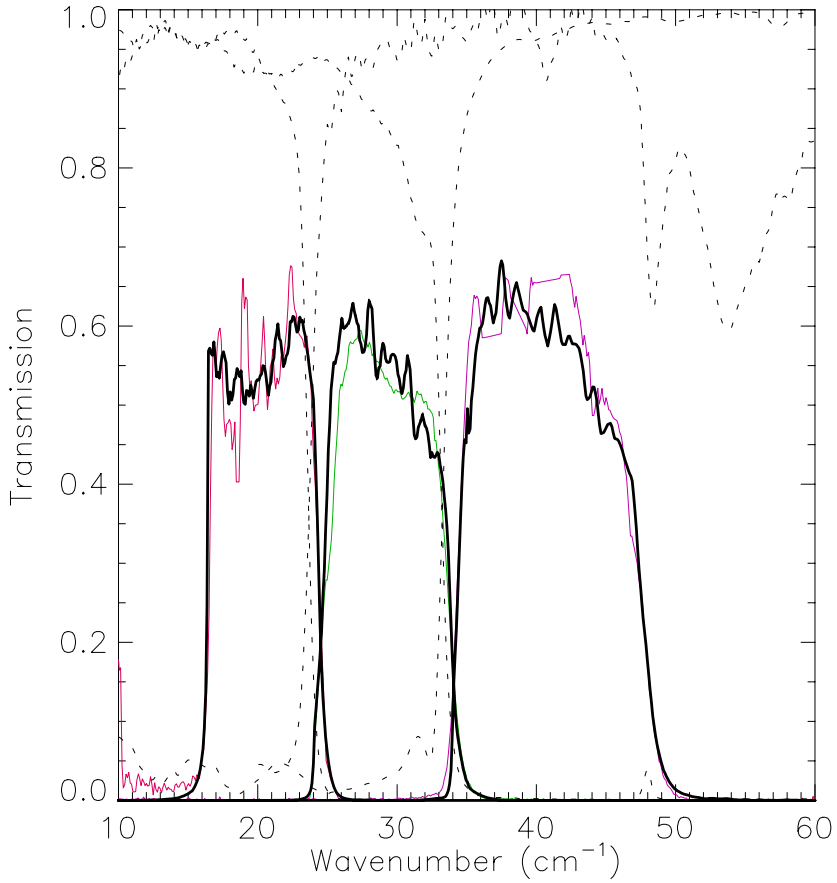

Figure 4.2-1: Average spectral bandpasses for SPIRE Photometer as measured during PFM4 (colours). Plotted with these are the filter profiles constructed from the individual laboratory measurements using shifted dichroic edges and nominal waveguide responses (dark black lines). The original positions of the dichroic measured bandpasses are shown in dashed lines. The waveguide cut-offs are modelled using the formulae in RD3.

4.3 Instrument-level requirements and their verification status.

IRD-OPTP-R05: Throughput

The throughput of the photometer mirrors, filters, dichroics and baffles shall be greater than 0.27 over the instrument waveband. This includes losses due to manufacturing defects; surface finish and alignment tolerances.

We can test the total throughput of the system by comparing the power absorbed by the detectors to that expected taking into account our knowledge of the instrument performance as measured or estimated from measurements of the individual components and theoretical expectations – table 4.3-1 gives the parameter values used

Table 4.3-1: Model Parameters for Photometer

Parameter	Where derived from	Value
Instrument spectral bandpass	Laboratory measurements of individual filters and feedhorn specification (RD3; RD6)	See figure 4.2-1
Detector optical efficiency	Taken from the BDA EIDP	Varies
Etendue (AΩ)	Theoretical expected for single mode	λ^2
Expected cold stop efficiency	Optical model	0.74
Loss due the hole in the BSM for PCAL	Metrology	0.95
Loss due to absorption and scattering from the mirrors	Estimate	0.995
Cold black body Emissivity	Estimate	1.0

Using loadcurves taken with the CBB at 9.7, 11.7 13 and 15 K we can measure the temperature rise and absorbed power in the detectors using the detector characteristics supplied in the EIDPs. Using the parameters in table 1 we integrate over the black body function to derive the expected absorbed power. The ratio of the measured and expected should be 1 if there are no unaccounted losses in the instrument. As and example of this comparison, figure 3.3-1 shows the expected and measured absorbed power versus CBB temperature (plotted as $\mathrm{Ln}(1/Q_{abs})$ vs $1/T_{CBB}$) for three sample photometer pixels. The measured power has been scaled by the average ratio between the measured and expected across all four CBB settings. This ratio is plotted for all pixels in figure 3.3-2. The values plotted here give the fractional variation between the model and the measurement. The discrepancies can arise for a number of reasons:

- CBB emissivity less than 1
- CBB flip mirror reflectivity lower than expected
- Throughput of the instrument less than expected

As a guide the expected throughput, taking an average filter transmission value, and not including the feedhorn efficiency, is:

PLW - 0.37
PMW - 0.36
PSW - 0.38

For PLW and PSW the central pixels have a ratio of ~0.8 measure/expected whereas PMW shows a ratio across the array of closer to 0.95. This would tend to argue against a common cause although this is not conclusive. The cause of the discrepancy is not understood at present and work on understanding it will continue. If we take the worst case then the throughput at the centres of the arrays is:

PLW - ~0.37x0.8 = 0.29

PMW - ~0.36x0.95= 0.34
PSW - ~0.38x0.8 = 0.30

These values drop to 0.26 at the unvignetted edge of PLW and 0.27 at the unvignetted edge of PSW. All bands therefore marginally meet the specification across most of the field of view even if the discrepancy seen is entirely due to a real loss in throughput.

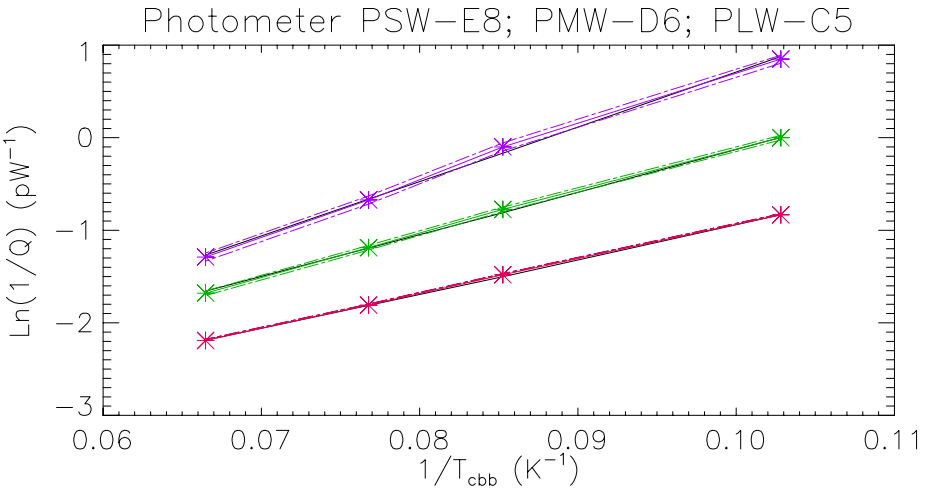

Figure 4.3-1: Example of measured and expected absorbed power derived from loadcurves with the CBB set to 9.7, 11.7,13 and 15 K. The straight black lines are the expected values, the coloured lines laid on top are the measured values with errors scaled by the mean of the Measured/Expected across all four CBB settings: PSW is purple, PMW green and PLW red. Note the agreement in the slope.

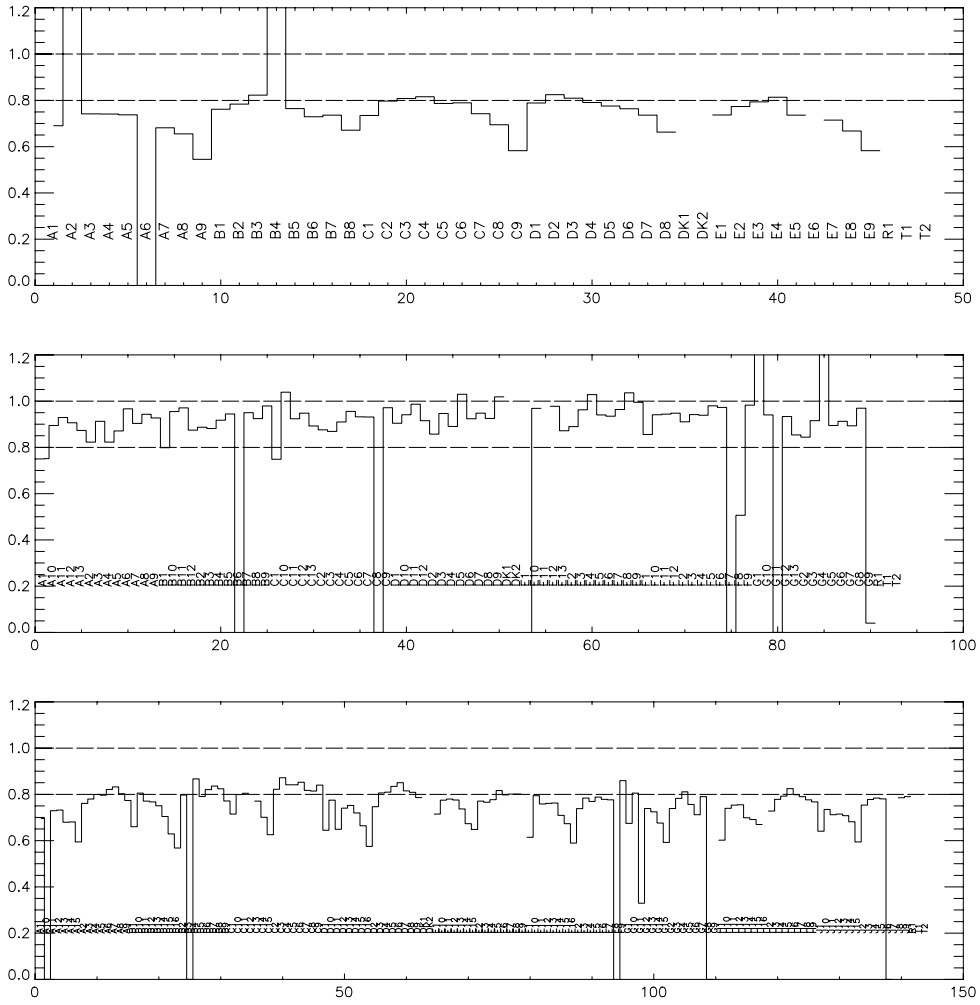

Figure 4.3-2: Ratio between measured and expected absorbed power onto the bolometers for PSW, PMW and PLW – top, middle and bottom respectively. These are taken as the mean of the ratios between the four CBB measurements shown in figure above. The dashed lines are to guide the eye and are set at 1.0 and 0.8.

IRD-OPTS-R05: Throughput

The theoretical throughput of the spectrometer mirrors; filters; beam splitters and baffles shall be greater than 0.2 over the total instrument waveband including all losses due to manufacturing defects; surface finish and alignment tolerances.

The same procedure as used for the photometer was carried out on the spectrometer during PFM1 testing. The bandpass and throughput assumptions are given here. The variation of the etendue with wavelength has now been firmly established using the beam data and associated analysis from PFM3 and PFM4 (see Optics Report RD5)

Table 4.3-2: Model Parameters for Spectrometer

Parameter	Where derived from	Value
Instrument spectral bandpass	Measurements of individual filters and feedhorn specification (RD3; RD6)	See figure 4.3-3 below
Detector optical efficiency	Taken from the BDA EIDP	Varies
Etendue (AΩ)	As derived from beam measurement data	SSW – 0.12 mm^2 sr independent of wavelength SLW - $4x10^{-6}.\lambda^2$ - $0.0045.\lambda + 1.65$ mm^2 sr
Expected cold stop efficiency	Optical model	0.75
Loss due the hole in the BSM for PCAL	Metrology	0.95
Loss due to absorption and scattering from the mirrors	Estimate	0.99
Reflectivity of the roof top mirror (2 surfaces)	Measured warm on alochromed mirror – this is a lower limit	0.81
Effective throughput due to not being at ZPD	Theory	0.5
Cold black body Emissivity	Estimate	1.0

The first check made was to see if we can reconstruct the spectral variation of a black body measurement using the model parameters listed above. Figure 4.3-3 shows an example of the derived transmission profile and expected profile from a measurement of the CBB after removal of the blackbody spectrum and the model etendue. Here we have chosen a value of the CBB temperature that does not saturate the detector but provides reasonable signal to noise in a single scan (no attempt at co-addition has been made).

As a further check we have derive the expected power per unit spectral interval by taking the transmission profile derived from one CBB temperature and applying to the other three. In the case of SLW the interferograms saturate for CBB temperatures above 10 K and for SSW the signal levels are very low for CBB temperatures below 10 K and the spectra will be prone to contamination by unaccounted straylight contributions. The results are compared to the expected spectra (including the etendue) in figure 4.3-4. Where the problems discussed here are not present, the absolute agreement is remarkable and we can confidently predict the static radiometric load onto the detectors.

Figure 4.3-5 shows the expected and measured absorbed power versus temperature for the spectrometer detectors in an analogous manner to the photometer shown in figure 4.3-1. The agreement here is not quite as good for SLW as the CBB temperature range used meant the SLW bolometer temperature range was large and caused problems with comparisons between cold and hot CBB cases. Figure 4.3-6 shows the average ratio between measured and expected absorbed power for all pixels. The SSW results are consistent and show ~1 at the centre of the array dropping to ~0.8 at the edges of the unvignetted area.

The SLW results show some scatter but the non-saturated and operational pixels show ratios >0.8 with the central pixel ~0.87. Examination of figure 4.3-3 shows that the implication of this is that the instruments meets specification over most of the waveband except for a region at the high frequency end of the band ~45 cm^{-1} (220 μm) upwards.

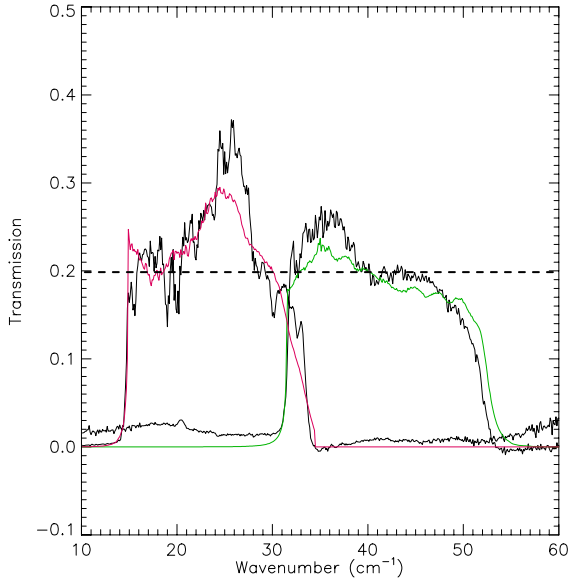

Figure 4.3-3: Derived transmission profiles for the central pixels (SLW-C3 and SSW-D4) compared to the stacked filter profiles. Here the waveguide diameters used are 0.3937 mm for SLW and 0.1860 mm for SSW. The dashed line represents the specification for the transmission.

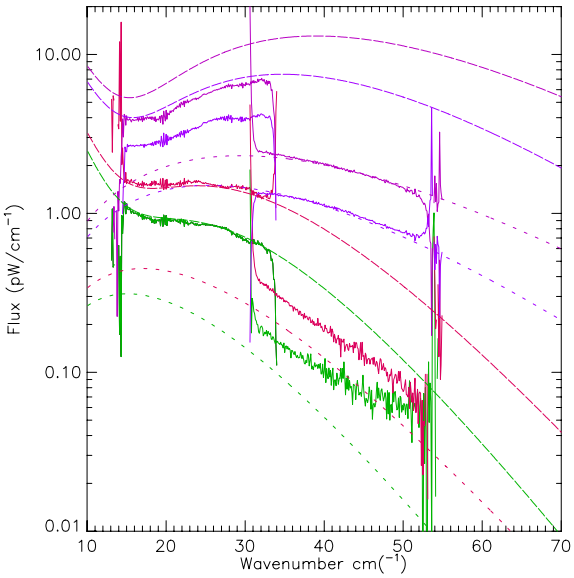

Figure 4.3-4: Recovered spectra for SLW-A1 and SSW-B5 in absolute units for the CBB at 7.7 (green), 8.7 (red), 13 (bluey-purple) and 15 K (purple). The SSW measured spectra are calibrated using the SSW 13-K derived transmission except for the 13-K data which use the 15-K derived transmission. The SLW data are calibrated using the 8.7-K derived transmission except the 8.7-K data which use the 7.7-K derived transmission. The long dashed lines are the predictions for SLW and the short dashed lines for SSW.

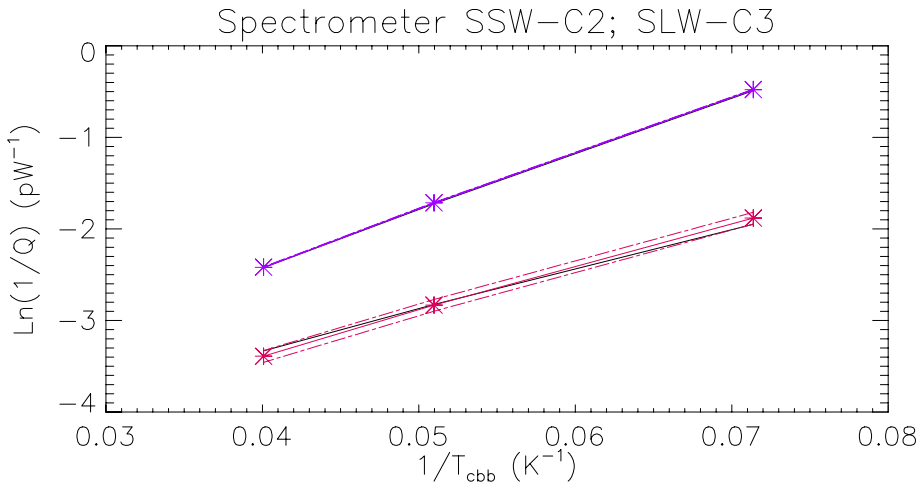

Figure 4.3-5: Example of measured and expected absorbed power derived from loadcurves with the CBB set to 14, 19.6 and 25 K. The straight black lines are the expected values, the coloured lines laid on top are the measured values with errors scaled by the mean of the Measured/Expected across all four CBB settings: SSW is purple and SLW red. Note the agreement in the slope for SSW and the disagreement for SLW. This is due to the large range in temperature seen by SLW bolometers over this range of CBB temperatures

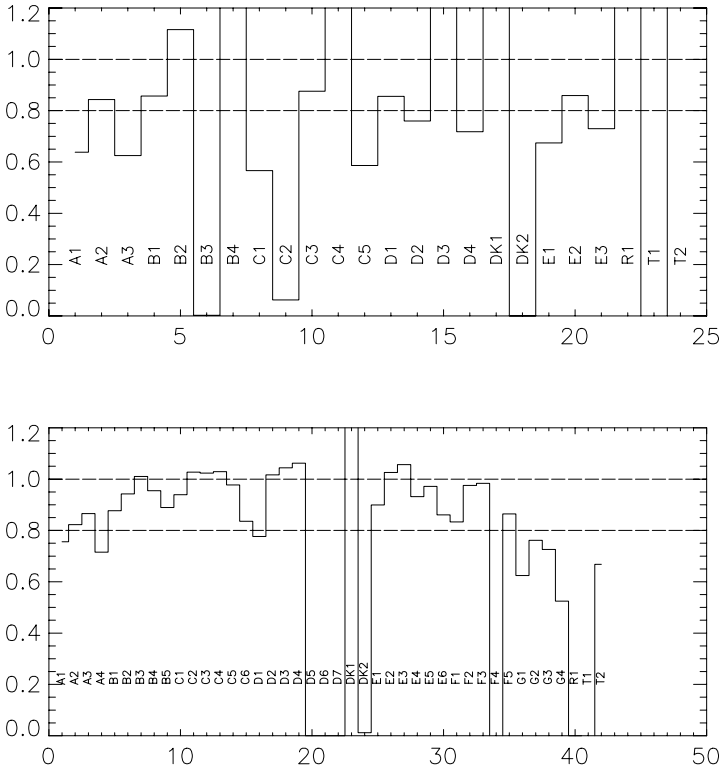

Figure 4.3-6: Ratio between measured and expected absorbed power onto the bolometers for SLW and SSW – top and bottom respectively. These are taken as the mean of the ratios between the four CBB measurements shown in figure 4.3-5. The dashed lines are to guide the eye and are set at 1.0 and 0.8.

SCAL port transmision

We have also tested the transmission to SCAL in a like manner by taking static photometric measurements at a number of SCAL4 temperatures. The model parameters for SCAL4 vary from those in table 4.3-2 only in the number of mirrors and filters in the optical train (RD6) and the effective emissivity of the source – set here to 0.04. Figure 4.3-7 shows the expected and measured absorbed power against temperature and 4.3-8 the calculated measured/expected ratio for each pixel. From 4.3-7 we can see that the emitted power is, as expected, more or less linear with temperature, however the ratio fo measured to expected is nearer to 2 – in fact greater than 2 – across much of the arrays. The reason for this is unknown at present and subject to further analysis.

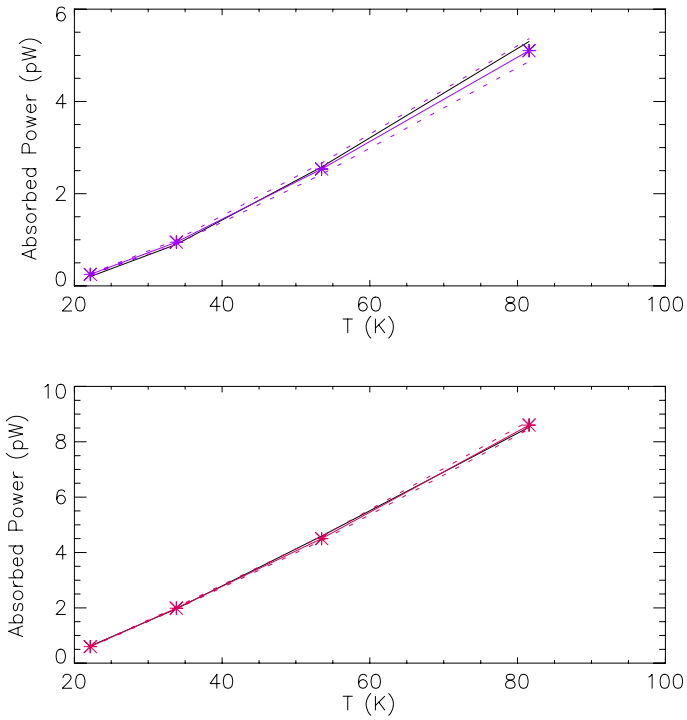

Figure 4.3-7: Absorbed power vs temperature for SCAL4 from loadcurve measurements. The expected power is in black and the measured, corrected using the average measured/expected ratio for all temperatures, is the coloured with stars. Note the plot is now Q vs T. Top is for SSW-C2 and bottom is for SLW-C3

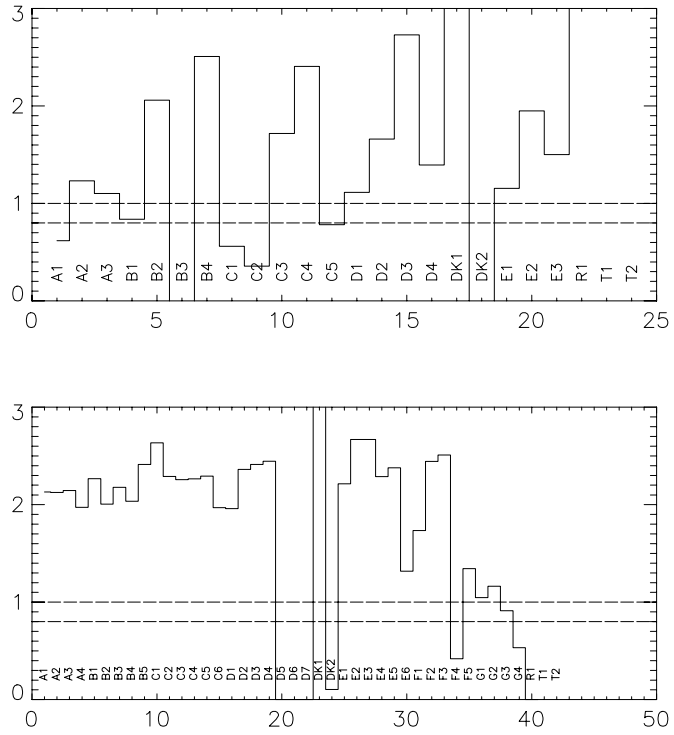

Figure 4.3-8: Ratio between measured and expected absorbed power onto the bolometers for SLW and SSW – top and bottom respectively. These are taken as the mean of the ratios between the four SCAL4 measurements shown in figure4.3-7. The dashed lines are to guide the eye and are set at 1.0 and 0.8.

5. Open Issues and Anomalies

These open issues from SVR-2 have now been closed

- The photometer bandpass is now well understood.
- The spectrometer etendue is now well modelled and on a firmer theoretical basis (see RD7)

The following open issues remain for further measurement/analysis

- The spectrometer bandpass as measured differs from that expected from the measured components. This requires further analysis to check the component measurements and produce high fidelity measured bandpass curves
- The transmission of the photometer may be lower than expected as indicated by the measurements from PFM4. This can be checked during system level testing using the cold cryostat lid.
- The transmission to the SCAL port as measured/modelled is clearly anomalous and the reason for this requires further analysis.

6. Recommendations for further data analysis and test

- Analysis of the spectra taken on the SCAL port
- Detailed comparison of the spectrometer bandpass against each component in the filter chain.
- Photometric measurements of the cryostat lid at various temperatures during the system level tests.